DEVELOPMENTAL DYNAMICS 238:2418–2429, 2009

Expression Analysis of *Sulf1* in the Chick Forebrain at Early and Late Stages of Development

Raquel García-López,[1] Cathy Soula,[2] and Salvador Martínez[1]*

***Sulfatase 1* is a secreted enzyme that modulates the sulfation state of heparan sulfate proteoglycans (HSPGs), which are potential key regulators of diverse developmental signals during embryonic patterning. In the present work, we have analyzed the *Sulf1* gene expression pattern during chicken forebrain development. Our results indicate that, at early developmental stages, chicken *Sulf1* is expressed in the alar and basal plate of the secondary prosencephalon (telencephalon and hypothalamus, respectively) as well as in the diencephalic basal and floor plates. Later in development, *Sulf1* is expressed by a subset of nuclei derived from these regions. *Developmental Dynamics 238:2418–2429, 2009.* © 2009 Wiley-Liss, Inc.**

Key words: *Sulf1*; prosencephalon; diencephalon; telencephalon; neural tube; sulfatase; oligodendrocyte

Accepted 9 June 2009

ABBREVIATIONS 3DM oculomotor nucleus, dorsomedial part **3v** third ventricle **AEP** entopeduncular area **AH** anterior hypothalamic area **APT** anterior pretectal nucleus **APTp** anterior pretectal nucleus, superficial cell plate **AuL1** auditory area of nidopallium, shell L1 field **Cb** cerebellum **ccs** caudocentral septal area **chp** choroid plexus **dCaPa** caudal paraventricular area, dorsal part **DIA** dorsal intermediate anterior nucleus of the thalamus **DIP** dorsal intermediate posterior nucleus of the thalamus **DLA** dorsolateral anterior nucleus of the thalamus **DMA** dorsomedial anterior nucleus of the thalamus **DMP** dorsomedial posterior nucleus of the thalamus **DPG** diffuse perigeniculate nucleus **DTgp1** dorsal tegmental area of prosomere 1 **ERot** epirotundic nucleus **ExM** external mammillary nucleus **Hb** habenular nucleus **HGF** hepatocyte growth factor **HPO** hypothalamic periventricular organ **Hyp** hypothalamus **IGL** intergeniculate leaflet **InC** interstitial nucleus of Cajal **IPT** intermediate pretectal nucleus **Is** isthmus **LA** lateral anterior hypothalamic nucleus **LHb** lateral habenular nucleus **LSHb** lateral subhabenular nucleus **LSt** lateral striatum **LTJ** lateral terminal nucleus, juxtacommissural part **M** mammillary nucleus **MCPI** magnocellular preisthmic nucleus **Mes** mesencephalon **MG** medial geniculate nucleus **MJC** medial juxtacommissural nucleus of the pretectum **MPG** medial perigeniculate nucleus **MPT** medial pretectal nucleus **MSHb** medial subhabenular nucleus **MV** mesopallium, ventral part **mVTA** mesencephalic ventral tegmental area **NIcp** nidopallium, intermediate part, corticoid plate **NIF** nidopallium, intermediate part, island field **OB** olfactory bulb **p1** prosomere 1 (pretectum) **p1MT** p1 medial terminal nucleus **p1PAG** p1 periaqueductal gray **p1PEW** p1 pre-Edinger-Westphal nucleus **p1Rt** p1 reticular formation **p1SNC** p1 substantia nigra, compact part **p1Tg** p1 tegmentum area **p1VTA** p1 ventral tegmental area **p2** prosomere 2 (thalamus) **p2PAG** p2 periaqueductal gray **p2Tg** p2 tegmentum area **p2VTA** p2 ventral tegmental area **p3** prosomere 3 (prethalamus) **p3Tg** p3 tegmentum area **p3VTA** p3 ventral tegmental area **pc** posterior commissure **Pe** periventricular stratum **PH** posterior hypothalamic nucleus **Pi** pineal gland **POA** preoptic area **PRot** perirotundic area **PrPT** principal pretectal nucleus of the commissural pretectum **PThB** basal prethalamic nucleus **Rh** rhombencephalon **rh1** rombomere 1 **RM** retromammillary nucleus **RMC** red nucleus, magnocellular part **Rot** rotundus nucleus **RPC** red nucleus, parvicellular part **SAC** stratum album centrale of the tectum **SCh** suprachiasmatic nucleus **Se** septum **SGC** stratum griseum centrale of the tectum **SGFS** stratum griseum et fibrosum superficiale of the tectum **SHb** subhabenular nucleus **SLPG** semilunar perigeniculate nucleus **sm** stria medullaris **SMi** superficial microcellular nucleus **SP** secondary prosencephalon **SPa** subparaventricular nucleus **SPC** superficial parvicellular nucleus of the thalamus **SpL** lateral spiriform nucleus **SPT** subpretectal nucleus **SRot** subrotundus nucleus of the thalamus **STh** subthalamic nucleus **TC** tuber cinereum area **TEL** telencephalom **TGC** tectal gray, central stratum **vCaPa** caudal paraventricular area, ventral part **VisCo** visual nidopallial nucleus, core region **VisSh** visual nidopallial nucleus, shell region **VTgM** ventral tegmental area of mammillary region **VTgp1** ventral tegmental area of prosomere 1 **VTgRM** ventral tegmental area of retromammillary region **xso** supraoptic decussation **ZLI** intrathalamic limitans zone

[1]Institute of Neuroscience UMH-CSIC, Campus de San Juan, San Juan, Alicante, Spain
[2]Université de Toulouse, UPS, Centre de Biologie du Développement, Toulouse, France
Grant sponsor: Marie Curie Training Sites; Grant number: QLK5-CT-2001.60029; Grant sponsor: European Union; Grant number: U.E. LSHG-CT-2004-512003 EUREXPRESS; Grant sponsor: ELA Foundation and Research Spanish grants; Grant number: BFU2008-0058; Grant number: CIBERSAM (CB07/09/0021); Grant number: INGENIO 2010 MEC-CONSOLIDER CSD2007-0002; Grant sponsor: Generalitat Valenciana; Grant number: CTDIA/2002/91; Bancaja.
***Correspondence to: Salvador Martínez, Instituto de Neurociencias, UMH-CSIC, Universidad Miguel Hernandez, Campus de San Juan, Carretera de Valencia, N-332, Km 87, E-03550, San Juan de Alicante, Spain. E-mail: smartinez@umh.es**

DOI 10.1002/dvdy.22039
Published online 3 August 2009 in Wiley InterScience (www.interscience.wiley.com).

INTRODUCTION

Heparan sulfate proteoglycans (HSPGs) are major components of the extracellular matrix that play a central role in controlling cell proliferation, differentiation, and morphological development through their interactions with signaling molecules and other extracellular matrix components (Perrimon and Bernfield, 2000; Selleck, 2000). HSPGs are composed of a protein core surrounded by covalently linked heparan sulfate (HS) chains composed of disaccharide repeats (Bernfield et al., 1999; Prydz and Dalen, 2000). Based on the nature of their core protein, they can be classified into three functionally distinct families: the transmembrane syndecans, the glycosylphosphatidylinositol (GPI) -anchored glypicans and the soluble perlecans. During synthesis of HS chains, a specific sulfation pattern of highly (S-domains), partially (transition zones), and nonsulfated regions is generated (Maccarana et al., 1996). This sulfation pattern is established in the Golgi apparatus by specific sulfotransferases at the 2-O position of uronic acid and 6-O, 3-O, and N positions of glucosamine (Ori et al., 2008). It has been proposed that this structural heterogeneity is specific of certain cell types or stages of development and plays an important role in regulating signaling pathways (Gallagher, 2006; Kreuger et al., 2006).

Recently, two additional HS-modifying enzymes that generate the sulfation HS pattern have been discovered. These enzymes, called Sulf1 and Sulf2, are extracellular endosulfatases that have the unique ability to eliminate the sulfate group in position 6-O of glucosamine in highly sulfated regions of HS (Morimoto-Tomita et al., 2002; Ai et al., 2003, 2007). Genes encoding for Sulf enzymes have been identified in birds, mouse, rat, and human, and more recently in amphibian (Dhoot et al., 2001; Morimoto-Tomita et al., 2002; Ohto et al., 2002; Braquart-Varnier et al., 2004; Nagamine et al., 2005; Ai et al. 2007; Freeman et al., 2008). During development, these enzymes are involved in regulating major signaling pathways, including Wnt, FGF, HGF, GDNF, BMP, and Shh (Dhoot et al., 2001; Ai et al., 2003; Wang et al., 2004; Viviano et al., 2004; Danesin et al., 2006, Ai et al., 2007, Freeman et al., 2008).

In the adult, deregulation of Sulf enzymes are involved in tumorigenesis (Lai et al., 2003; Nawroth et al., 2007; Narita et al., 2007).

During development, Sulf proteins are expressed in neural and mesodermal tissues (Dhoot et al., 2001, Wang et al., 2004; Braquart-Varnier et al., 2004; Danesin et al., 2006; Ai et al., 2007). In the embryonic central nervous system (CNS), *Sulf1* has been shown to be expressed in floor plate cells and in a subset of neural progenitors of the spinal cord, as well as in the choroid plexus (Dhoot et al., 2001; Ohto et al., 2002; Braquart-Varnier et al., 2004). In the ventral spinal cord, *Sulf1* has been detected in oligodendrocyte progenitors, where it functions as a positive regulator of Shh signaling and contributes to trigger neural progenitors from a neuronal to glial fate (Danesin et al., 2006).

In this study, we have performed a detailed analysis of *Sulf1* expression in the forebrain of chicken embryo. We have further compared *Sulf1* expression with previously described genes such as *Nkx2.2*, *plp/dm20*, and *Pax6* to precisely position domains of *Sulf1* expression within the longitudinal as well as transversal prosomeric limits. Our analysis is based on the prosomeric model developed by L. Puelles, J.R.L. Rubenstein, and coworkers (Bulfone et al., 1993; Puelles and Rubentein, 1993; Puelles, 1995; Rubenstein et al., 1998; Puelles and Rubenstein, 2003). In this model, the anteroposterior (AP) regionalization first causes the forebrain to become subdivided into rostral secondary prosencephalon (hypothalamo-telencephalic complex) and caudal diencephalon (Puelles et al., 1987, 2004; Puelles and Rubenstein, 1993, 2003; Puelles, 1995). The diencephalic region next develops three prosomeric transverse units, known as prosomeres 1–3 (p1–p3; Puelles and Rubenstein, 2003). Our results show a markedly regional pattern of *Sulf1* expression throughout forebrain development.

RESULTS

We first described the early gene expression pattern of *Sulf1* at Hamburger and Hamilton (HH) stages HH10 (embryonic day [E] 2) to HH26 (E5) in whole-mounts. Next, we analyzed in consecutive series of coronal sections the molecular pattern at later stages (E8 (HH34), E14 (HH 40), and E18 (HH44)). Representative results are displayed in Figure 1 for earlier stages and Figures 2–6 for later stages. We have used the anatomical nomenclature and abbreviations of the Chick Brain Atlas by Puelles et al., 2007 (see the list of abbreviations).

Sulf1 Gene Expression at Early Stages (HH10–HH26)

Sulf1 transcripts were first detected at stage HH10 (E2) in the mesoderm adjacent to the hindbrain (Fig. 1A). In the CNS, *Sulf1*-expressing cells were first observed at stage HH18 (E2.5; Fig. 1B).

At E2.5–E3 (HH18–HH20), *Sulf1* expression was exclusively localized in the roof plate of the telencephalon and in the basal plate of the diencephalon, mesencephalon and rostral rhombencephalon (Fig. 1B–D). Even though it is expressed in the floor plate of the spinal cord, caudal rhombencephalon, (r2–r7) and diencephalon, *Sulf1* transcripts were absent in the floor plates of the rostral rhombencephalon (r1) and mesencephalon (where the expression shifted from the floor to basal plate), as well as in the whole isthmic region, between r1 and mesencephalon (Fig. 1D).

At E4 and E5 (HH22–HH26), the expression pattern of *Sulf1* changed significantly. Rostrally, new regions with *Sulf1* + cells appeared inside the secondary prosencephalon: in the choroid plexus at the roof plate (chp; Fig. 1E–G), as well as in the preoptic region (POA; Fig. 1F,G), subparaventricular area (SPa; Fig. 1E–H), and the caudal paraventricular areas (dCaPa, vCaPa; Fig. 1F,H), in the alar plate.

Ventrally, in the basal plate, *Sulf1* was expressed in mammillary area (M; Fig. 1F–H), as well as in the mammillary and retromammillary regions of the ventral tegmental area (VTgM, VTgRM; Fig. 1E–H). Note the weak *Sulf1* signal in the dorsal retromammillary area (RM; Fig. 1E–H).

In the diencephalon, at E4.5 and E5 (HH24–HH26), *Sulf1* signal was lo-

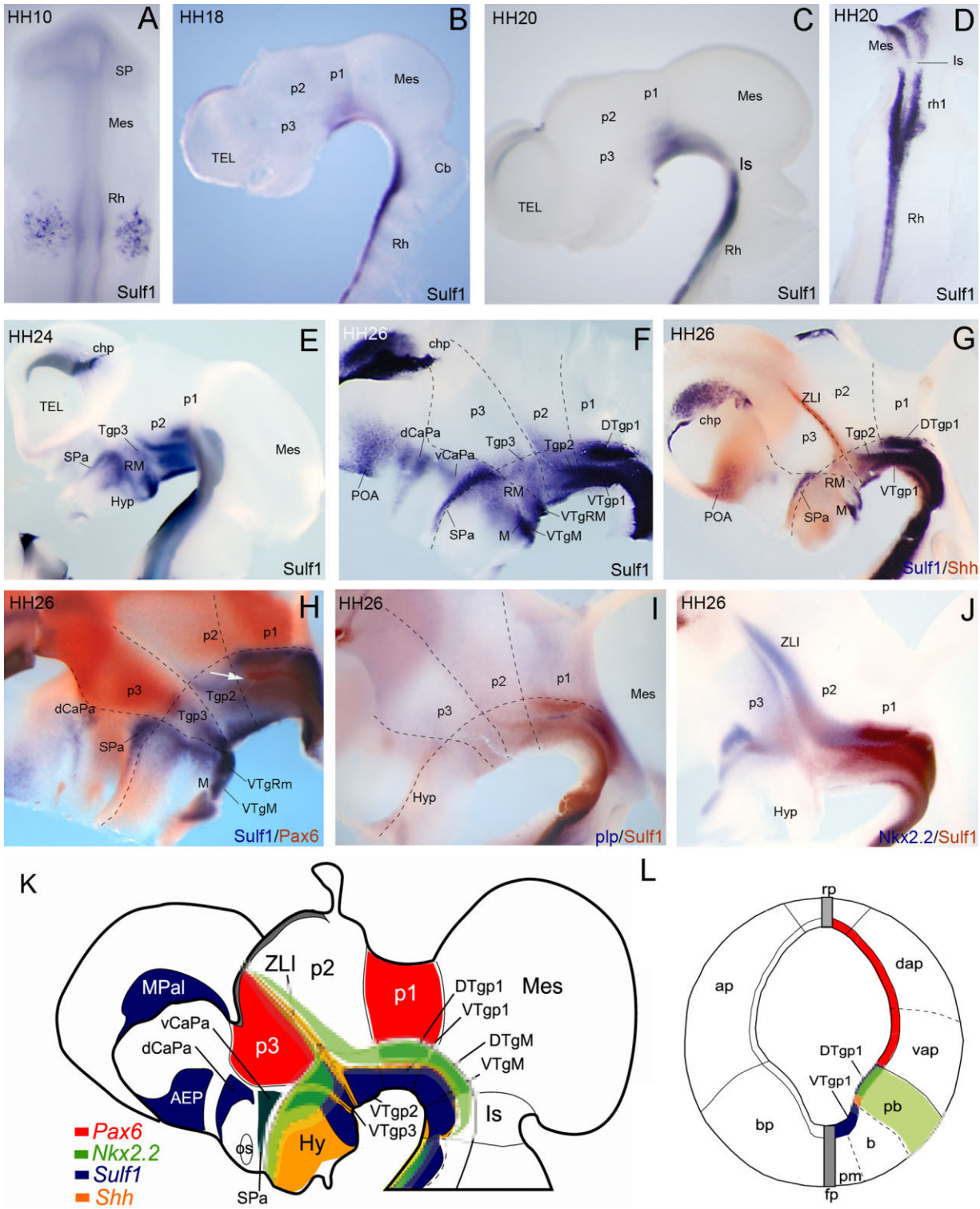

Fig. 1. A–J: Expression of *Sulf1* at early stages of neural tube development (A,D: anterior is up; B,C,E–J: anterior is oriented to the left). Whole-mount chick embryos at embryonic day (E) 2 (HH10; A), E2.5 (HH18; B), E3 (HH20; C,D), E4.5 (HH24; E), and E5 (HH26; F–J). **A:** Dorsal view of the chick neural tube at HH10. **B,C:** Lateral view of the chick neural tube at HH18 and HH20. **D:** Dorsal view of the rombencephalon at HH20. **E:** In situ hybridization of *Sulf1* at stage HH24. **F:** Lateral view of a chick neural tube at HH26. **G,H:** Double in situ hybridization with *Sulf1* (labeled in blue) and *Shh* (G), *Pax6* (H; labeled in red). **I,J:** Double in situ hybridization with *Sulf1* (labeled in red) and *plp/dm20* (I), *Nkx2.2* (J; labeled in blue). The dashed lines identify the interprosomeric boundaries (transversal oriented lines) and the alar–basal limit (longitudinal oriented line). **K:** Schematic representation of expression patterns in a lateral view of neural tube at stage HH24, color codes represent the expression patterns of *Nkx2.2*, *Pax6*, *Shh*, and *Sulf1*. **L:** Diagram of a section transversal to p1. b, basal plate; dap, dorsal alar plate; fp, floor plate; pb, parabasal plate; pm; paramedian band; rf, roof plate; vap, ventral alar plate.

calized only in ventral domains. Strong expression appeared in the floor and basal plates of p1 and p2, whereas in p3 the signal was weaker (Fig. 1E–J). Double in situ hybridization with *Sulf1* (labeled in blue) and *Shh* (labeled in red) showed that *Sulf1* expression was absent in the zona limitans intrathalamica (ZLI), a *Shh*-expressing domain that separates the prethalamus and thalamus (p3/p2 boundary; Bulfone et al., 1993; Puelles and Rubenstein, 1993; Fig. 1G). A *Sulf1* weak area was detected, corresponding to p3 tegmentum (Tgp3), which was limited caudally by a negative strip, separating Tgp3 from the p2-positive tegmentum (Tgp2). This strip continued the p3/p2 limit into the basal and roof plates of the diencephalon (Fig. 1F–H). Note that in prosomere 2, we observed a *Sulf1* weakly expressing domain progressing from the basal plate into the alar plate, ending caudal to the ZLI in the anteroventral region of the thalamus (Fig. 1F). In prosomere 1 (p1), *Sulf1* selectively labeled an additional band dorsal to the continuous tegmental expression in p1 (VTgp1) and p2 (Tgp2; Fig. 1E–J). At these early stages of development, the alar/basal boundary in p1 is underlined by the ventral edge of *Pax6* expression in the alar plate; and the dorsal border of *Nkx2.2* expression in the parabasal band of the basal plate (Puelles et al., 2000; Ferran et al., 2007). Thus, to adequately localize the DTgp1 band, we carried out double in situ hybridization for *Sulf1* and *Nkx2.2*, *plp/dm20*, or *Pax6*. Pretectal *Pax6* transcripts appeared in the entire alar plate adjacent to the alar–basal boundary, while an additional positive strip appeared separated in the basal mantle layer (Fig.1H; Ferran et al., 2007). Double in situ hybridization with *Sulf1* (labeled in blue) and *Pax6* (labeled in red) showed that the basal *Pax6* + cell band appeared ventral to the DTgp1 *Sulf1*-positive band (between DTgp1 and VTgp1; arrow in Fig. 1H). In addition, it is interesting to note how the strong expression of *Pax6* in the alar plate of p3 allows clear identification of this domain and recognition of its corresponding basal region, between two weak *Sulf1*-expressing stripes. While the anterior limit of basal p3 was localized between VTgRM and Tgp3, its caudal limit coursed between Tgp3 and Tgp2 (Fig. 1H). When double in situ hybridization with *plp/dm20* (labeled in blue) and *Sulf1* (labeled in red) was performed, *plp/dm20* signal appeared ventral to the DTgp1-positive band (Fig. 1I). Finally, comparison of *Nkx2.2* (labeled in blue) and *Sulf1* (labeled in red) expression patterns showed that DTgp1 overlapped with the dorsal part of the *Nkx2.2*-expressing band (Fig. 1J). We then developed a *Sulf1* expression maps in relation to *Shh*, *Pax6*, *plp/dm20*, and *Nkx2.2* expression patterns between stages HH24 and HH26 (Fig. 1K,L).

Sulf1 Gene Expression at Later Stages in the Telencephalon

While the early expression of *Sulf1* in the telencephalon was restricted to the roof plate, presumptive region of the choroid plexus and the septum (Pombero and Martinez, 2009), new areas appeared in the subpallium at HH26 (E5): the POA and Pa. Then, between E8 (HH34) and E18 (HH44), we observed new pallial domains expressing *Sulf1* in the telencephalon.

Telencephalic Pallium

Regional specific expression in the ventral pallium

The ventral pallium (VPall) corresponds to the old "neostriatum" and was recently renamed as "nidopallium" (Reiner et al., 2004). The ventral pallium includes, rostrally, the olfactory bulb and several associated areas. The olfactory bulb strongly expressed *Sulf1* in the mitral cell layer (Fig. 2E,F). The VPall encloses several thalamorecipient nuclear formations, as well as associative areas, classified as nidopallial subregions (Puelles et al., 2000, 2007; Reiner et al., 2004), including the so-called island fields (Redies et al., 2001). High level of *Sulf1* expression was found at the intermediate and caudal nidopallium whereas the frontal areas of VPall appeared negative for *Sulf1*. On the other hand, the intermediate nidopallium presents the visual core nuclei (VisCo), corresponding to the old "ectostriatum," or "entopallium" of Reiner et al. (2004). The entire complex, consisting of a core portion (VisCo) plus an associative shell (VisSh), strongly expressed *Sulf1* at E12 (HH38, data not shown) and at later stages (E14, HH40 and E18, HH44; Fig. 2E–G,I,J). The nidopallial island field (NIF) that surrounds VisCo also showed some positive *Sulf1*-expressing islands (Fig. 2F,I,J). In the caudomedial part of the VPall (caudal nidopallium), we detected the auditory core nucleus and its associative shell formation (AuL), a large ovoid region classically called "L field." AuL1 domain strongly expressed *Sulf1* at E18 (HH44) while AuL2 and AuL3 expression levels were less intense and irregular (AuL1; Fig. 2K,L).

Regional specific expression in the lateral pallium

The lateral pallium, adjacent to dorsal pallium, and previously known as "ventral hyperstriatum," was recently renamed mesopallium (Reiner et al., 2004; Puelles et al., 2007). In the mesopallium, *Sulf1* was transiently expressed in the anterior areas of its ventral and dorsal parts (MV; Fig. 2E–G). This signal was only observed at E14 (HH40) and disappeared at E18 (HH44, Fig. 2I–L).

Expression in the Telencephalic Subpallium

The subpallium derivatives develop into the striatal, pallidal-peduncular, and preoptic regions (Puelles et al., 2000, 2004, 2007). In the striatum, we observed scattered *Sulf1*+ cells in its lateral part (LSt; Fig. 2H,K), while, in the septum (Se), located in the medial telencephalic wall, ependymal expression of *Sulf1* was detected at all stages analyzed (Fig. 2A–C,H–K).

Sulf1 Gene Expression at Later Stages in the Hypothalamus

The hypothalamus forms the non-telencephalic region of the secondary prosencephalon (Puelles et al., 1987, 2004, 2007; Puelles, 1995, 2001a; Puelles and Rubenstein, 2003). Most of the caudal hypothalamic ventricular epithelium strongly expressed *Sulf1*, with the exception of the floor plate that appeared negative except

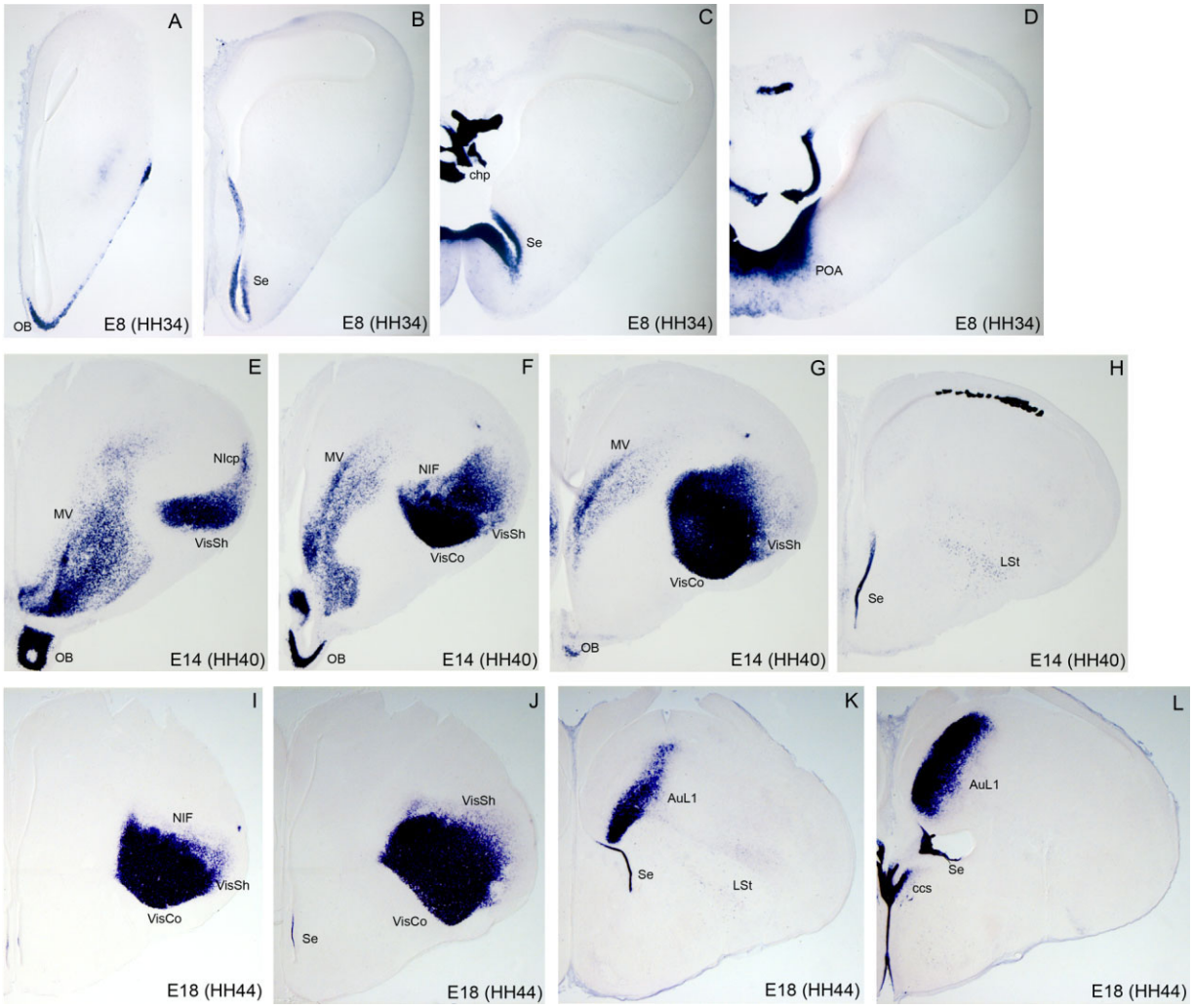

Fig. 2.

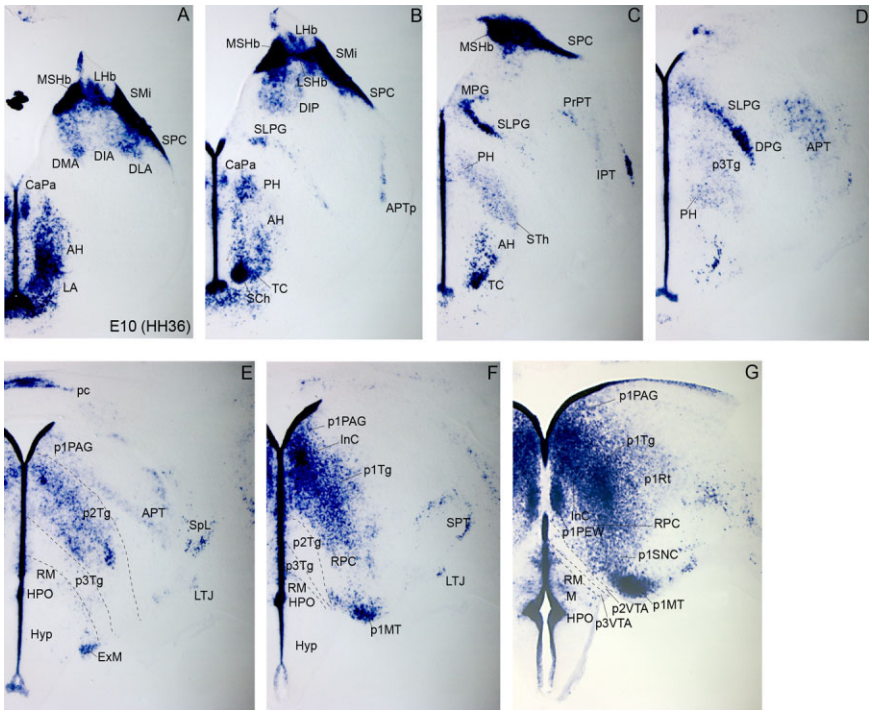

Fig. 3.

Fig. 2. In situ hybridization of *Sulf1* expression in the chick telencephalon. **A–L:** Coronal sections at embryonic day (E) 8 (HH34; A–D), E14 (HH40; E–H), and E18 (HH44; I–L) are shown in a rostral-to-caudal sequence and dorsal is to the top. Whereas in early stages of development (E8), *Sulf1* is mainly detected in the subpallial and olfactory bulb neuroepithelium (A–D), later in development (E–L) *Sulf1* becomes activated in the extended telencephalic pallial derivatives of ventral pallium (VisCo, VisSh, and AuL1) and lateral pallium (MV).

Fig. 3. A–G: In situ hybridization of *Sulf1* in E10 (HH36) chick brains, showing coronal sections from rostral (A) to caudal levels (G). Basal plate ependymal cells strongly express *Sulf1*, together with abundant cells in the hypothalamus, diencephalic and mesencephalic tegmental areas. A–C: Dorsally, in the alar plate, strong expression of *Sulf1* was detected in the habenular region, where ependymal cells of the subhabenular nucleus (SHb) were strongly positive. A–C: From this SHb region, a superficial stream of *Sulf1*-expressing cells forms the SMi and SPC nuclei. C–F: Some pretectal nuclei contain *Sulf1*-expressing cells. Dashed lines in E–G delimit the interprosomeric boundaries in diencephalic tegmental regions.

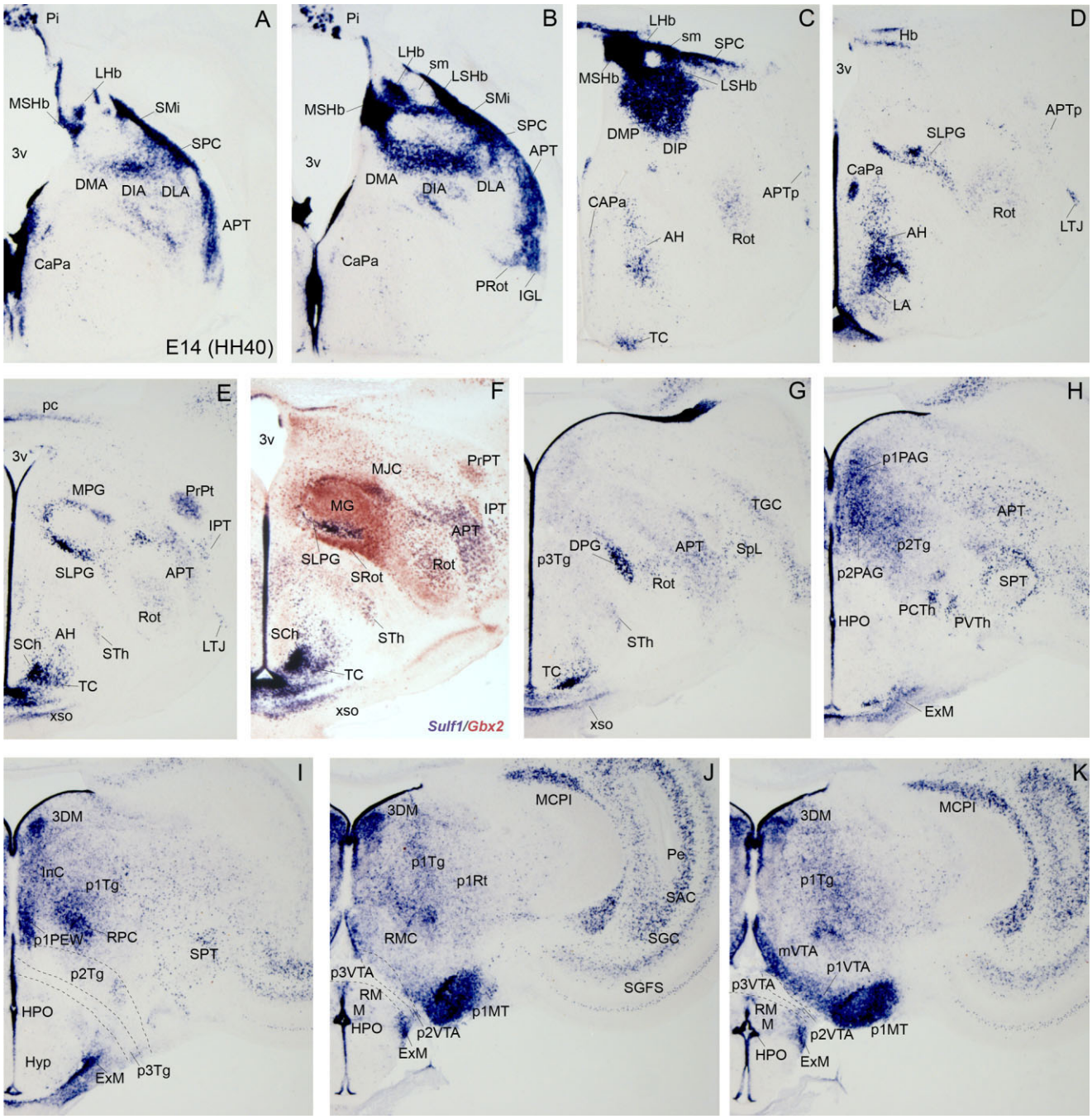

Fig. 4. **A–K:** Coronal sections at embryonic day 14 (HH40), showing rostral (A) to caudal (K); (A–E,G–K) hybridized for *Sulf1* and (F) depicts double in situ hybridization with *Sulf1* (labeled in blue) and *Gbx2* (labeled in red). Both ependymal and nuclear cells maintain *Sulf1* expression in this more mature stage of development. F: *Gbx2* expression allows to better localize and identify *Sulf1* expression in the thalamus.

for the mammilar region (MM). In addition, several nuclei in the mantle layer expressed this gene.

Regional specific expression in the alar hypothalamus

The alar hypothalamus is divided longitudinally into an upper optopeduncular paraventricular area and a subparaventricular area underneath (Puelles et al., 2007). Maintaining the early expression domains, *Sulf1* transcripts were detected in subparaventricular ependymal cells, crossing the midline at the level of the posterior supraoptic decusation (xsod; Figs. 3B–D, 4E–I, 5B). In the mantle layer, we observed *Sulf1* expression in the caudal paraventricular nucleus (CaPa; Figs. 3A,B, 4C,D, 5A) and the suprachiasmatic nucleus (SCh; Puelles et al., 2007; Figs. 3B, 4E,F; 5B,C). Moreover, at the analyzed stages (E10, E14, and E18), we also observed *Sulf1*+ cells in the tuber cinereum area (TC; Figs. 3B,C, 4E, 5B–F), anterior hypothalamic area (AH; Figs. 3A–C, 4C–E, 5A,B), and lateral anterior hypothalamic nucleus (LA; Figs. 3A, 4D, 5A).

Regional specific expression in the basal hypothalamus

The basal hypothalamus is divided into the rostral or prepeduncular hypothalamic domain and caudal or peduncular hypothalamic domain (Puelles et al., 2007). In the prepeduncular domain *Sulf1* expression was not detected, whereas some nuclei of the peduncular domain expressed *Sulf1* during these stages: the hypothalamic periventricular organ strongly expressed *Sulf1* (HPO; Figs. 3E–G, 4H–K, 5F,H). Finally, while the medial mammillary nuclei (MM) presented a weak signal, high level of *Sulf1* expression was detected in the external mammillary nucleus (ExM) at these stages (Figs. 3E, 4I–K, 5G). We have also observed *Sulf1* + cells in the subthalamic nucleus (STh; Figs. 3C, 4E–G, 5B–E).

Sulf1 Gene Expression at Later Stages in the Diencephalon

According to the prosomeric model, the diencephalon proper represents the continuation of the forebrain caudal to the hypothalamus, down to the border with the midbrain (Puelles and Rubenstein, 2003; Puelles et al., 2004). The diencephalic region develops three segments or neuromeres, known as prosomeres 1–3 (p1 lying caudally, adjacent to the midbrain, and p3 rostrally, contacting the hypothalamus and the telencephalon; Puelles et al., 1987; Puelles and Rubenstein, 2003). Each prosomere displays characteristic dorsal and ventral domains, namely, the dorsalized roof and alar plates and the ventralized basal and floor plates. The alar territory produces three anatomical regions: alar p1 = pretectum; alar p2 = thalamus and habenula (the old dorsal thalamus and epithalamus); alar p3 = prethalamus (prior ventral thalamus; see fate map in García-López et al., 2004).

Regional specific expression in Prosomere 3

Prethalamus (alar plate). The prethalamus was negative for *Sulf1* in the analyzed stages (from E8, HH34 to E18, HH44; Figs. 4A–G, 5A–F).

Prethalamic tegmentum (basal and floor plates). In the reticular tegmentum (p3Tg; Puelles et al., 2007), weak expression of *Sulf1* was detected at E10 (HH36, Fig. 3D), where at later stages (E14, HH40 and E18, HH44) the signal disappeared (Figs. 4G, 5D) except from the most anterior ventral tegmental area (p3VTA; Fig. 4K). Otherwise, p3 ependymal tegmentum was strongly positive for *Sulf1* transcripts (Fig. 3E–G).

Regional specific expression in Prosomere 2

Thalamus (alar plate). This large nuclear complex can be subdivided into 5 main histogenetic areas (Redies et al., 2000; Puelles, 2001b; Martínez-de-la-Torre et al., 2002; García-López et al., 2004). These areas are the habenular/subhabenular complex or epithalamus, the dorsal tier group, the intermediate tier group, the ventral tier group, and the anteroventral group (Redies et al., 2000; Puelles, 2001b; Martinez-de-la-Torre et al., 2002; Puelles et al., 2007).

In the *habenular/subhabenular* complex, *Sulf1* was strongly expressed in the subhabenular ependymal region, the lateral and medial subhabenular nuclei (LSHb, MSHb), as well as in the periventricular stratum and lateral habenular nucleus (LHb; Figs. 3A–C, 4A–C, 5A,B).

Ventral to the subhabenular nuclei appears the *dorsal tier domain*, which produces a voluminous mass of derivates in its mantle layer that represent the largest components of the avian thalamus (Redies et al., 2000; Puelles, 2001b; Puelles et al., 2007). High levels of *Sulf1* expression was detected in several of the nuclear components in the dorsal tier: dorsomedial anterior (DMA; Figs. 3A, 4A–C, 5A), dorsal intermediate anterior and posterior nuclei (DIA, DIP; Figs. 3A,B, 4A–C, 5A,B) and in the dorsolateral anterior nuclei (DLA; Figs. 3A, 4A,B, 5A). Superficially, a continuous stream of *Sulf1*-expressing cells was observed from the subhabenular nuclei to the superficial parvicellular nucleus (SPC; Figs. 3A–C, 4A–C, 5B) and in the superficial microcellular nucleus (SMi; Figs. 3A,B, 4A,B, 5A,B).

The *intermediate tier* is larger caudally, where it makes extensive contact with the pretectum (Redies et al., 2000; Puelles, 2001b; Martínez-de-la-Torre et al., 2002; Puelles et al., 2007). In this tier, *Sulf1* expression was restricted to the largest part of this complex, the rotundus nucleus (Rot), which is pushed outward ventrolaterally by the disproportionate growth of the dorsal tier group. Faint *Sulf1* expression in the scattered rotundic cell was detected at stage E12 (HH38, data not shown). At E14 (HH40), the low level of *Sulf1* expression was apparent (Fig. 4C–G) but at E18 (HH44), we observed high expression levels compared with previous stages (Fig. 5B–E).

Ventral to the intermediate tier is a smaller histogenetic domain called the *ventral tier*. This domain contains the avian medial geniculate nucleus (MG, Puelles et al., 2007), formerly called "ovoidal nucleus" (Papez, 1935, 1936). It is surrounded by inner and outer perigeniculate formations: medial perigeniculate nucleus (MPG) and semilunar perigeniculate nucleus (SLPG). To better locate *Sulf1* expression in the intermediate and ventral thalamic tiers, we carried out double in situ hybridization experiments for *Sulf1* (labeled in blue) and *Gbx2* (labeled in red). *Gbx2* was strongly expressed in the ventral tier derivatives (i.e., the MG) and in the subrotundus nucleus (SRot; Puelles et al., 2007), a derivative of the anteroventral area (Martinez-de-la-Torre et al., 2002). We observed that the MG and SRot, stained with the *Gbx2* probe, were negative for *Sulf1* (positive for *Gbx2*, Fig. 4F) while MPG and SLPG were strongly positive (Figs. 3B–D, 4D–F, 5B,C). In addition, the diffuse perigenulate area also expressed *Sulf1* (DPG; Figs. 3D, 4G, 5D,E).

In the chicken, cells originating in the boomerang-shaped *anteroventral histogenetic zone* of the dorsal thalamus migrate to the surface, partially filling the area of origin in depth and partially dispersing tangential-caudally in the superficial strata of p2, to finally cover the most of the dorsal, intermediate, and ventral tiers (Rendahl, 1924; Puelles et al., 1991; Yoon et al., 2000; Puelles et al., 2007). The known derivatives of this region (subrotundus nucleus, perirotundic area and intergeniculate leaflet) differentiate in close spatial relation to the rotundus nucleus. The expression of *Sulf1* was restricted at the perirotundic area (PRot), pirotundic nucleus

(ERot; Puelles et al., 1991), and intergeniculate leaflet (IGL; Figs. 4B, 5A,D). The complex formed by IGL plus PRot corresponds to the "n.superficialis magnocellularis" of Rendahl (1924). This was then renamed "n.interstitialis tractus opticus" by Puelles et al. (1991) and Martínez et al. (1991). Also, we observed expression in the posteroventral and posterocaudal thalamic nuclei (PVTh, PCTh; Figs. 4H, 5F).

Thalamic tegmentum (basal and floor plates). *Sulf1* was expressed in the basal p2 epithelium as well as in disperse reticular cells of the thalamic tegmentum (p2Tg), including the anterior pole of the ventral tegmental area (p2VTA; Figs. 3E, 4H).

Regional specific expression in Prosomere 1

Prosomere 1 consists of the pretectal region in its alar plate, as well as a distinct underlying tegmental region.

Pretectum (alar plate). The pretectum is wedged between the thalamic portion of the diencephalon and the midbrain. The alar pretectum appears anteroposteriorly divided into three main radial histogenetic areas called commissural (PTc), juxtacommissural (PTj), and precommissural domains (PTp; Yoon et al., 2000; Redies et al., 2000; Puelles et al., 2007; Ferran et al., 2007). These terms refer to their positions relative to the posterior commissure. The sets of nuclei derived from the three subdivisions of the pretectum displayed differences regarding to *Sulf1* expression.

Commissural pretectum. We mapped *Sulf1*-positive cells in migrated nuclei of the commissural domain, the principal pretectal nucleus (PrPT; Puelles et al., 2007), the intermediate pretectal nucleus (IPT; Puelles et al., 2007), and subpretectal nucleus (SPT; Puelles et al., 2007; Figs. 3C–F, 4E,F,H,I, 5D–H).

Juxtacommissural pretectum. *Sulf1* expression was prominent in the medial juxtacommisural nucleus (MJC; Figs. 4F, 5E), and scattered cells of the lateral spiriform nucleus (SpL; Figs. 3E, 4G, 5F), as well as the juxtacommissural portion of the lateral terminal nucleus of the accessory optic tract

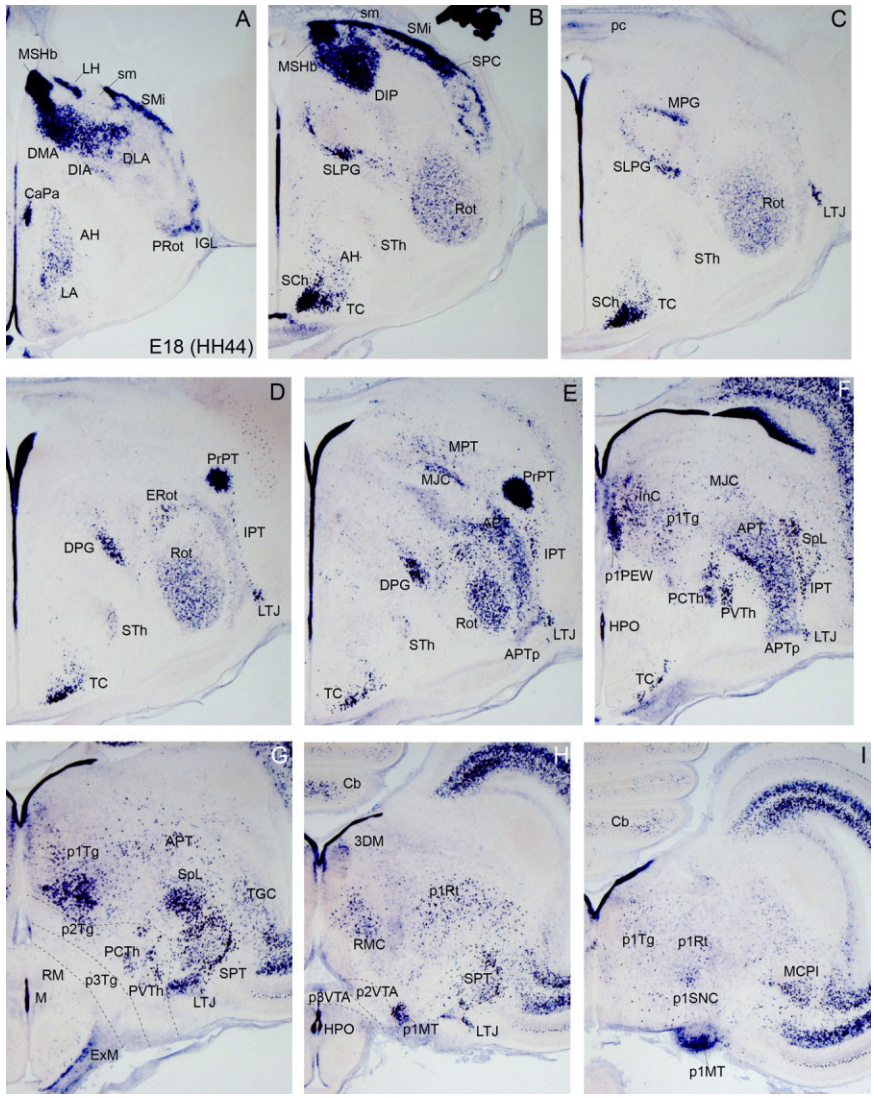

Fig. 5. **A–I:** In situ hybridization of *Sulf1* expression in embryonic day (E) 18 (HH44) chick brain, showing rostral (A) to caudal (I) levels. Both ependymal and nuclear cells maintain *Sulf1* expression in this more mature stage of development. In addition to increasing the complexity of expression domains in relation to the higher complexity in diencephalic and pretectal nuclear structure, PrPT appears now strongly positive for *Sulf1* transcripts.

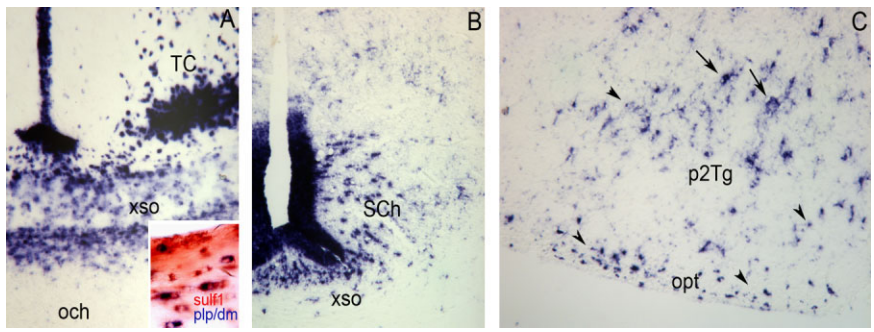

Fig. 6. A–C: In situ hybridization of *Sulf1* in paraffin coronary sections at embryonic day (E) 8 (HH34). **A:** High power micrograph showing *Sulf1*-positive cells in the hypothalamus, apparently cells migrating into the supraoptic (xso) and optic chiasm (och) commissures, and into the tuber cineruem (TC) nuclei. The insert represent cells in the supraoptic commissure in a E18 chick brain co-expressing *Sulf1* in red and *plp/dm20* in blue. **B,C:** While *Sulf1*-expressing cells into the axonal tracts and some in nuclear areas are small (arrowheads in C), such as oligodendrocytes, large cells in the central-most hypothalamic mantle layer (arrows in C) seems to corresponds to neurons.

(LTJ; Puelles et al., 2007; Figs. 3E,F, 4D,E, 5C–H).

Precommissural pretectum. *Sulf1* was especially prominent in cells of the anterior pretectal nucleus (APT; prior "principal precommissural nucleus"; Figs. 3D,E, 4E–H). We also observed weak *Sulf1* expression in two layers of the previously known-as "superficial synencephalic nucleus," the superficial cell plate of the APT (APTp; Puelles et al., 2007; Figs. 3B, 4C,D) and superficial plexiform layer of the APT (APTs; Puelles et al., 2007; Figs. 4B,C, 5C). *Sulf1* was strongly expressed in the p1 portion of the medial terminal nucleus of the accessory optic tract (p1MT; Puelles et al., 2007; Figs. 3G, 4J, 5H,I). The MT in birds was named "n.ectomammillaris" or "n. of the basal optic root" (Puelles et al., 2007). We also detected high levels of *Sulf1* expression in the interstitial nucleus of Cajal (InC; Puelles et al., 2007; Figs. 3F, 4I, 5F).

Pretectal tegmentum (basal and floor plates). *Sulf1* was strongly expressed throughout all p1 tegmentum (p1Tg; Puelles et al., 2007): the parvocellular red nucleus (RPC), the p1 reticular formation (p1Rt), the p1 pre-Edinger-Westphal nucleus (p1PEW), the p1 substantia nigra, pars compacta (p1SNC), and the p1 ventral tegmental area (p1VTA; Figs. 3E–G, 4H–K, 5F–I).

Phenotype of *Sulf1* Expressing Cells

While early expression was localized in the neural tube epithelium, *Sulf1*-expressing cells migrated and differentiated in various regions of the neural parenchyma. We then studied the mature morphological phenotype of *Sulf*-expressing cells. Epithelial expression was retained in the majority of the basal plate ependymal areas: caudal hypothalamus, diencephalon, and mesencephalon. Even though interprosomeric limits were evident at early stages of development (Fig. 1E,F,H,K), we did not detect clear differences or heterogeneities in the ependymal expression at later stages of development. In contrast to the strong homogeneous expression in ependymocytes, mantle layer cells varied in size, morphology, and distribution. Small *Sulf1*-positive cells that invaded the axonal tracts from positive ependymal regions were strongly reminiscent of oligodendrocyte progenitors (Fig. 6A,C), while the second population of cells, much larger in size and with polygonal cell bodies, was distributed in nuclear areas, suggesting that they could be neurons (Fig. 6B).

DISCUSSION

Sulf1 Expression at Early Stages

In the present study, we have addressed the precise distribution of *Sulf1* transcripts during forebrain development in chick embryos. At early stages, our in situ hybridization experiments revealed a restricted pattern of *Sulf1* expression in the neural tube. Rostrally, in the secondary prosencephalon, the expression pattern was distributed in alar and basal neuroepithelial domains, while in the diencephalon *Sulf1* expression was restricted to the basal plate epithelium. Although *Sulf1* expression in the basal plate, telencephalic POA and SPa could be directly related to the regulation of *Shh* signaling due to the expression of both genes in nearby domains (Puelles et al., 2007; Bardet, 2007; García-López et al., 2008), *Sulf1* expression throughout the choroids plexus (chp) seems to be unrelated to Shh signaling.

In the diencephalic prosomeres, the *Sulf1* signal was restricted to basal plate domains and was weakly expressed at the level of interprosomeric boundaries. This expression pattern is evidence that there is a continuity of the interprosomeric boundaries, which were easily detectable in the alar plate, into the basal plate. Thus, *Sulf1* expression in the basal plate brings additional evidence supporting the segmental character of diencephalic prosomeres and its metameric structure, and clearly argues against alternative interpretation in favor of a columnar distribution of the basal plate diencephalic neuroepithelium (Larsen et al., 2001).

In this work, we compared the expression of *Sulf1* with that of *Nkx2.2*, *plp/dm20*, and *Pax6*, by double in situ hybridization to precisely locate *Sulf1*-positive bands in prosomere 1 according to recent studies on pretectal regionalization (Ferran et al., 2007). The issue of molecularly defining the alar–basal boundary at diencephalic levels is still open for discussion. Shimamura and collaborators (1995), Puelles and Rubenstein (1993, 2003), and Puelles and collaborators (2004) tentatively postulated that the longitudinal band of progenitor cells expressing *Nkx2.2* "approximates" the alar–basal boundary. Moreover, Ferran and collaborators (2007) recently observed that the molecular alar–basal diencephalic boundary corresponds to the limit between the *Pax6* expression domain in the alar plate neuroepithelium and the *Nkx2.2* expression domain in the basal plate. In this study, we observed that the dorsal *Sulf1*+ band only present in p1 appeared ventrally compared with the dorsal Pax6-expressing domain, and partially overlapped with the *Nkx2.2* domain. Accordingly, we have assumed in the present report that this Sulf1+ band in prosomere 1 is localized in the basal plate.

Whether *Sulf1* is involved in oligodendroglial specification in chick brain remains an open question. In support of this, we observed that *Sulf1* expression in the *Nkx2.2* domain of the ventral brain neuroepithelium, starting from E4, is earlier than the specification of oligodendrocyte progenitors in this territory and co-expression of both genes in migrated oligodendrocyte precursors. However, we do not observe any overlap between the *plp/dm20* domain of expression and *Sulf1*-positive bands in prosomere 1. In the chick developing brain, the ventricular domains of *plp/dm20* expression correspond to restricted foci that give rise to oligodendrocytes, closely associated to the domain of Shh expression (Poncet et al., 1996; Pringle et al., 1996; Perez-Villegas et al., 1999). In mouse, *PDGFR*α and *plp/dm20* have been shown to be expressed in distinct oligodendroglial precursors (Spassky et al., 1988); therefore, we cannot exclude that *plp/dm20* and *Sulf1* identify distinct neural precursors with oligodendroglial potential. Thus, in the rostral part of the CNS, such *Sulf1*$^{+}$*/plp-dm20*$^{-}$ precursors may coexist with *Sulf1*$^{-}$*/plp-dm20*$^{+}$ precursor cells. In chick, the positional information that controls the pattern of specification of neural stem cells has to account for mosaic-like patterns inside the ventral segments of the CNS. An

explanatory model for such a mosaic pattern of specification has already been proposed for different subtypes of motor- and interneurons, which segregate within contiguous columnar domains along the ventrodorsal axis of the neuroepithelium (Pfaff et al., 1996; Ericson et al., 1997), as well as of neurons and oligodendrocytes in the diencephalon from *plp/dm20*-positive progenitors (Spassky et al., 2008).

Sulf1 Expression at Late Stages of Development

At late stages of development, *Sulf1* was highly expressed in ependymal regions of the corresponding *Sulf1*-expressing neuroepithelial domains. In the alar plate, in addition to choroidal and septal expression, *Sulf1* appeared in the ependymal regions of ventral habenular nuclei. This epithalamic expression, together with the choroidal plexus, represents exceptions to the topological relation between *Shh* and *Sulf1*-expressing domains (Ericson et al., 1995; Vieira et al., 2005).

From these epithelial domains, *Sulf1*-positive cells further invaded different levels of the mantle layer, following migratory routes and entering into the axonal tracts (mainly small cells that suggest to be oligodendroglia progenitors) or nuclear neuropiles (with heterogeneous sizes and shapes, possibly neuronal and glial fates).

In the telencephalon, the in situ hybridization study revealed a restricted pattern of *Sulf1* expression into a subset of gray matter structures:

In the *ventral pallium*, intense gene expressions was detected in the intermediate and caudal nidopallium (VisCo, VisSh, NIF, AuL; Reiner et al., 2004).The nidopallium is a large hypopallial neuronal mass that contains a variety of sensorial nuclei receiving specific thalamic inputs (old ectostriatum, now called entopallium in Reiner et al., 2004, or VisCo in Puelles et al., 2007; L field , actually AuL; and n. basalis, now BSS in Puelles et al., 2007), surrounded by "associative" populations.

Lateral pallium derivatives, classically termed hyperstriatum ventrale, recently renamed mesopallium (Reiner et al., 2004), was described as constituted by dorsal and ventral areas (HVd; HVv; Huber and Crosby, 1926; Karten and Hodos, 1967). In our study, we observed transient *Sulf1* expression in anterior regions of the mesopallium.

Subpallium.

We followed in our description the radial subdomains recently defined in Puelles and collaborators (2007), showing *Sulf1* expression pattern in the septum (Se) and weak expression in the lateral striatal area (LSt).

With the exception of the septum, the rest of the telencephalon did not present ependymal *Sulf1*-expressing territories, suggesting that its expression has been upregulated in cells when they have already migrated into the mantle layer. Although no evident relationship between this pattern of expression and Shh signaling can be proposed, we do not exclude a possible function for *Sulf1* in modulating Shh signaling in these cells. Indeed, Shh has recently been identified as a trophic signal for different neuronal populations in the telencephalon and cerebellum (Komada et al., 2008; revised in Vaillant and Monard, 2009).

In the *alar hypothalamus*, cells from the subparaventricular primordium (SPa) migrate into the overlying paraventricular nucleus complex, forming the resulting paraventricular core nucleus (PaCo; Puelles, 2000). Our data suggest that *Sulf1*-expressing cells migrate from SPa to invade the tuber cinereum area (TC), anterior hypothalamic area (AH), and lateral anterior hypothalamic nucleus (LA).

In the *basal hypothalamus*, we detected *Sulf1*-expressing cells in the subthalamic nucleus (STh). The avian STh is clearly an homolog of the mammalian nucleus of the same name (Jiao et al., 2000). STh originates from the retromammillary pouch, and its cells migrate dorsally briefly (Puelles et al., 2007).

The *diencephalic* domain is subdivided into three segments or neuromeres, known as prosomeres 1, 2, and 3 (Puelles et al., 1987, 2007; Puelles and Rubenstein, 2003). In prosomere 1 and 2 regions, we observed intense *Sulf1* expression in alar and basal territories. In prosomere 3, we observed a *Sulf1*-negative alar domain as well as a weak signal at stage E10 (HH36). While an abundant amount of *Sulf1*-expressing cells, which would correspond to locally produced oligodendroglial progenitors and reticular neurons, were detected in the basal plates, the heterogeneous alar expression could represent both migrated *Sulf1*-positive cells from the basal plate or local *Sulf1* activation. A recent clonal study of *plp/dm20* cell distribution in developing mouse thalamus showed a generation of both alar and basal diencephalic neuronal and glial cells from the basal domain expressing this gene (Delaunay et al., 2009). Functional studies are now required to define the function of *Sulf1* in the differentiation and functional maturation of thalamic cells.

The expression of *Sulf1* in the neural tube and spinal cord has been previously reported both in quail and rat (Dhoot et al., 2001; Ohto et al., 2002). In chick, *Sulf1* expression was detected in ventral neuroepithelial cells of the spinal cord (Braquart-Varnier et al., 2004). This study suggests that *Sulf1* could represent a gene expressed by cells of the oligodendroglial lineage: both in oligodendrocyte neuroepithelial progenitors and in more mature oligodendrocytes. In the embryonic chick spinal cord, the specification of oligodendroglial precursors in the basal plate requires the morphogenetic signal of Sonic hedgehog (Shh) produced by the notochord and floor plate cells (Trousse et al., 1995; Orentas and Miller, 1996; Poncet et al., 1996; Braquart-Varnier et al., 2004; Danesin et al., 2006). Moreover, the creation of oligodendrocyte precursors from ventral Nkx2.2-expressing neural progenitors occur precisely when these progenitors stop generating neurons, indicating that the mechanism of the neuronal/oligodendroglial switch is a time related feature that is most likely dependent of ventral specification. Chick-*Sulf1* is expressed in the ventral neuroepithelium of the spinal cord just before oligodendrocyte specification and seems to be involved in the regulation of Shh signaling (Danesin et al., 2006).

EXPERIMENTAL PROCEDURES

Chick Embryos

Fertilized chicken eggs (*Gallus gallus domesticus*) were obtained from commercial sources and incubated at 37°C in a forced air incubator until the desired embryonic stage. The embryos were staged according to Hamburger and Hamilton (1951).

In Situ Hybridization to Whole-Mount Embryos or to Tissue Sections

The head of the chick embryos was fixed overnight by immersion in 4% paraformaldehyde in phosphate-buffered saline solution (PBS; 0.1 M, pH 7.4). In addition, E18 embryos were transcardially perfused with the same fixative solution. All brains were dissected out and post-fixed for 48 hr at 4°C. Early embryos (HH10–HH26) were processed as whole-mounts, whereas the brains of older embryos (HH33–HH44) were dissected, embedded in 4% agarose in PBS, and transversally sectioned in 100-μm-thick sections with a Vibratome (Leica). Several embryos were embedded in paraffin and 8 μm were obtained.

In Situ Hybridization

Antisense digoxigenin-labeled riboprobes for *Sulf1*, *Gbx2*, *Pax6*, *plp/dm20*, *Nkx2.2*, and *Shh* were synthesized and subsequently processed for in situ hybridization as previously described by Henrique and collaborators (1995). RNA labeled probes were detected by an alkaline-phosphatase-coupled antibody (Roche Diagnostics, Mannheim, Germany), and NBT/BCIP (nitroblue tetrazolium/5-bromo-4-chloro-3-indolyl phosphate) were used as a chromogenic substrate for the alkaline phosphatase (Boehringer, Mannheim, Germany). Several whole-mounts and floating sections were processed for two-color, double hybridization using digoxigenin (dig)- and fluorescein (f)-labeled antisense riboprobes for *Sulf1* and either *Shh*, *Gbx2*, *Nkx2.2*, *Pax6*, or *plp-dm20*. The digoxigenin-labeled probes were revealed in dark blue using an NBT/BCIP solution, whereas the fluorescein-labeled probes were revealed in red, using an INT/BCIP solution, following a standard procedure. After hybridization, embryos were washed in PBT, photographed under a dissecting microscope (Leica) and stored at 4°C in PBT/0.1% sodium azide.

ACKNOWLEDGMENTS

We thank Nathalie Escalas for her help in Toulouse and Dr. Jonathan Jones his help in revising our manuscript.

REFERENCES

Ai X, Do AT, Lozynska O, Kusche-Gullberg M, Lindahl U, Emerson CP Jr. 2003. Qsulf1 remodels the 6-O sulfation states of cell surface heparan sulfate proteoglycans to promote Wnt signaling. J Cell Biol 162:341–351.

Ai X, Kitazawa T, Do AT, Kusche-Gullberg M, Labosky PA, Emerson CP Jr. 2007. SULF1 and SULF2 regulate heparin sulfate-mediated GDNF signalling for esophageal innervation. Development 134:3327–3338.

Bardet S. 2007. Organización morfológica y citogenética del hipotálamo del pollo sobre base de mapas moleculares. Tesis doctoral. Universidad de Murcia.

Bernfield M, Gotte M, Park PW, Reizes O, Fitzgerald ML, Lincecum J, Zako M. 1999. Functions of cell surface heparin sulphate proteoglycans. Annu Rev Biochem 68:729–777.

Braquart-Varnier C, Danesin C, Clouscard-Martinato C, Agius E, Escalas N, Benazeraf B, Ai X, Emerson C, Cochard P, Soula C. 2004. A subtractive approach to characterize genes with regionalized expression in the gliogenic ventral neuroepithelium: identification of chick Sulfatase 1 as a new oligodendrocyte lineage gene. Mol Cell Neurosci 25:612–628.

Bulfone A, Puelles L, Porteus MH, Frohman MA, Martin GR, Rubenstein JL. 1993. Spatially restricted expression of Dlx-1, Dlx-2 (Tes-1), Gbx-2, and Wnt-3 in the embryonic day 12.5 mouse forebrain defines potential transverse and longitudinal segmental boundaries. J Neurosci 13:3155–3172.

Danesin C, Agius E, Escalas N, Ai X, Emerson C, Cochard P, Soula C. 2006. Ventral neural progenitors switvh toward an oligodendroglial fate in response to increased Sonic hedgehog (Shh) activity: involvement of Sulfatase 1 in modulating Shh signalling in the ventral spinal cord. J Neurosci 26:5037–5048.

Delaunay D, Heydon K, Miguez A, Schwab M, Nave KA, Thomas JL, Spassky N, Martinez S, Zalc B. 2009.Genetic tracing of subpopulation neurons in the prethalamus of mice (Mus musculus). J Comp Neurol 512:74–83.

Dhoot GK, Gustafsson MK, Ai X, Sun W, Standiford DM, Emerson CP Jr. 2001. Regulation of Wnt signaling and embryo patterning by an extracellular sulfatase. Science 293:1663–1666.

Ericson J, Muhr J, Jessell TM, Edlund T. 1995. Sonic hedgehog: a common signal for ventral patterning along the rostrocaudal axis of the neural tube [review]. Int J Dev Biol 39:809–816.

Ericson J, Rashbass P, Schedl A, Brenner-Morton S, Kawakami A, van Heyningen V, Jessell TM, Briscoe J. 1997. Pax6 controls progenitor cell identity and neural fate in response to graded Shh signalling. Cell 90:169–180.

Ferran JL, Sanchez-Arrones L, Sandoval JE, Puelles L. 2007. A model of early molecular regionalization in the chicken embryonic pretectum. J Comp Neurol 481:42–57.

Freeman SD, Moore WM, Guiral EC, Holme AD, Turnbull JE, Pownall ME. 2008. Extracellular regulation of developmental cell signaling by XtSulf1. Dev Biol 320:436–445.

Gallagher JT. 2006. Multiprotein signalling complexes: regional assembly on heparin sulphate [review]. Biochem Soc Trans 34:438–441.

García-López R, Vieira C, Echevarria D, Martinez S. 2004. Fate map of the diencephalon and the zona limitans at the 10-somites stage in chick embryos. Dev Biol 268:514–530.

García-López M, Abellán A, Legaz I, Rubenstein JL, Puelles L, Medina L. 2008. Histogenetic compartments of the mouse centromedial and extended amygdala based on gene expression patterns during development. J Comp Neurol 506:46–74.

Hamburger V, Hamilton HL. 1951. A series of normal stages in the development of the chick embryo. J Morphol 88:49–92.

Henrique D, Adam J, Kyat A, Chitnis A, Lewis J, Ish-Horowicz D. 1995. Expression of a Delta homologue in prospective neurons in the chick. Nature 375:787–790.

Huber GC, Crosby EC. 1926. On thalamic and tectal nuclei and fiber paths in the brain of the American alligator. J Comp Neurol 40:97–227.

Jiao Y, Medina L, Veenman CL, Toledo C, Puelles L, Reiner A. 2000. Identification of the anterior nucleus of the ansa lenticularis in birds as the homolog of the mammalian subthalamic nucleus. J Neurosci 20:6998–7010.

Karten HJ, Hodos W. 1967. A stereotaxic atlas of the brain of the pigeon, Columba livia. Baltimore: The Johns Hopkins University Press.

Komada M, Saitsu H, Kinboshi M, Miura T, Shiota K, Ishibashi M. 2008. Hedgehog signaling is involved in development of the neocortex. Development 135:2717–2727.

Kreuger J, Spillmann D, Li JP, Lindahl U. 2006. Interactions between heparin sulfate and proteins: the concept of specificity [review]. J Cell Biol 174:323–327.

Lai J, Chien J, Staub J, Avula R, Greene EL, Matthews TA, Smith DI, Kaufmann SH, Roberts LR, Shridhar V. 2003. Loss of HSulf1–1 upregulates heparin-binding growth factor signalling in cancer. J Biol Chem 278:23107–23117.

Larsen CW, Zeltser LM, Lumsden A. 2001. Boundary formation and compartition in the avian diencephalons. J Neurosci 21:4699–4711.

Maccarana M, Sakura Y, Tawada A, Yoshida K, Lindahl U. 1996. Domain structure of heparan sulfates from bovine organs. J Biol Chem 271:17804–17810.

Martínez S, Wassef M, Alvarado-Mallart RM. 1991. Induction of a mesencephalic phenotype in the 2-day-old chick prosencephalon is preceded by the early expression of the homeobox gene en. Neuron 6:971–981.

Martínez-de-la-Torre M, Garda AL, Puelles E, Puelles L. 2002. Gbx2 expres-

sion in the late embryonic chick dorsal thalamus. Brain Res Bull 57:435–438.
Morimoto-Tomita M, Uchimura K, Werb Z, Hemmerich S, Rosen SD. 2002. Cloning and characterization of two extracellular heparin-degrading endosulfatases in mice and humans. J Biol Chem 277:49175–49185.
Nagamine S, Koike S, Keino-Masu K, Masu M. 2005. Expression of a heparin sulphate remodelling enzyme, heparin sulphate 6-O-endosulfatase sulfatase FP2, in the rat nervous system. Dev Brain Res 159:135–143.
Nawroth R, van Zante A, Cervantes S, McManus M, Hebrok M, Rosen SD. 2007. Extracellular sulfateses, elements of the Wnt signalling pathway, positively refulate growth and tumorigenicity of human pancreatic cancer cells. PLoS ONE 2:392.
Narita K, Chien J, Mullany SA, Staub J, Qian X, Lingle WL, Shridhar V. 2007. Loss of HSulf-1 expression enhances autocrine signalling mediated by amphiregulin in breast cancer. J Biol Chem 282:14413–14420.
Ohto T, Uchida H, Yamazaki H, Keino-Masu K, Matsui A, Masu M. 2002. Identification of a novel nonlysosomal sulphatase expressed in the floor plate, choroid plexos and cartilage. Genes Cells 7:173–185.
Ori A, Wilkinson MC, Fernig DG. 2008. The heparanome and regulation of cell function: structures, functions and challenges [review]. Front Biosci 13:4309–4338.
Orentas DM, Miller RH. 1996. A novel form of migration of glial precursors. Glia 16:27–39.
Papez JW. 1935. Thalamus of turtles and thalamic evolution. J Comp Neurol 61: 433–475.
Papez JW. 1936. Evolution of the medial geniculate body. J Comp Neurol 64:41–61.
Perez-Villegas EM, Olivier C, Spassky N, Poncet C, Cohard P, Zalc B, Thomas JL, Martinez S. 1999. Early specifications of oligodendrocytes in the chick embryonic brain. Dev Biol 216:98-113.
Perrimon N, Bernfield M. 2000. Specificities of heparin sulphate proteoglycans in developmental processes. Nature 404: 725–728.
Pfaff SL, Mendelsohn M, Stewart CL, Edlund T, Jessell TM. 1996. Requirement for LIM homeobox gene IsI1 in motor neuron generation reveals a motor neuron-dependent step in interneuron differentiation. Cell 84:309-320.
Pombero A, Martinez S. 2009. Telencephalic morphogenesis during the process of neurulation. An experimental study using quail-chick chimeras. J Comp Neurol 512:784–797.
Poncet C, Soula C, Trousse F, Kan P, Hirsinger E, Pourquié O, Duprat AM, Cochard P. 1996. Induction of oligodendrocyte progenitors in the trunk neural tube by ventralizing signals: effects of notochord and floor plate grafts, and of sonic hedgehog. Mech Dev 60:13–32.
Pringle NP, Yu W, Guthrie S, Roelink H, Lumsden A, Peterson A. 1996. Determination of neuroepithelial cells fate: induction of the oligodendrocyte lineage by ventral midline cells and Sonic hedgehog. Dev Biol 177:30-42.
Prydz K, Dalen KT. 2000. Synthesis and sorting of proteoglycans. J Cell Sci 113: 193–205.
Puelles L. 1995. A segmental morphological paradigm for understanding vertebrate forebrains. Brain Behav Evol 46: 319–337.
Puelles E. 2000. Patrón de expression génica e histogénesis en la placa basal de prosencéfalo y mesencéfalo de aves. Tesis doctoral. Universidad de Murcia.
Puelles L. 2001a. Brain segmentation and forebrain development in amniotes. Brain Res Bull 55:695–710.
Puelles L. 2001b. Thoughts in the development, structure and evolution of the mammalian and avian telencephalic pallium, Philos Trans R Soc Lond B Biol Sci 356:1583–1598.
Puelles L, Rubenstein JL. 1993. Expression patterns of homeobox and other putative regulatory genes in the embryonic mouse forebrain suggest a neuromeric organization. Trends Neurosci 16:472–479.
Puelles L, Rubenstein JL. 2003. Forebrain gene expression domains and the evolving prosomeric model. Trends Neurosci 26:469–476.
Puelles L, Amat JA, Martínez-de-la-Torre M. 1987. Segment-related, mosaic neurogenetic pattern in the forebrain and mesencephalon of early chick embryos: I. Topography of AChE-positive neuroblasts up to stage HH18. J Comp Neurol 266: 247–268.
Puelles L, Guillén M, Martinez-de-la-Torre M. 1991. Observations on the fate of nucleus superficiales magnocellularis of Rendahl in the avian diencephalon, bearing on the organization and nomenclatura of neighboring retinorecipient nuclei. Anat Embryol (Berl) 183:221–233.
Puelles L, Kuwana E, Puelles E, Bulfone A, Shimamura K, Keleher J, Smiga S, Rubenstein JRL. 2000. Pallial and subpallial derivatives in the embryonic chick and mouse telencephalon, traced by the experession of the genes Dlx-2, Emx-1, Nkx-2.1, Pax-6, and Tbr-1. J Comp Neurol 424:409–438.
Puelles L, Martinez S, Martinez-de-la-Torre M, Rubenstein JLR. 2004. Gene maps and related histogenetic domains in the forebrain and midbrain. In: Paxinos G, editor. The rat nervous system, 3rd ed. San Diego: Academic Press.
Puelles L, Martinez-de-la-Torre M, Paxinos G, Watson CH, Martinez S. 2007. The chick brain. In stereotaxic coordinates. An atlas featuring neuromeric subdivisions and mammalian homologies. New York: Academic Press.
Redies C, Ast M, Nakagawa S, Takeichi M, Martínez-de-la-Torre M, Puelles L. 2000. Morphologic fate of diencephalic prosomeres and their subdivisions revealed by mapping cadherin expression. J Comp Neurol 421:481–514.
Redies C, Medina L, Puelles L. 2001. Cadherin expression by embryonic divisions and derived gray matter structures in the telencephalon of the chicken. J Comp Neurol 438:253–285.
Reiner A, Perkel DJ, Bruce LL, Butler AB, Csillag A, Kuenzel W, Medina L, Paxinos G, Shimizu T, Striedter G, Wild M, Ball GF, Durand S, Gunturkun O, Lee DW, Mello CV, Powers A, White SA, Hough G, Kubikova L, Smulders TV, Wada K, Dugas-Ford J, Husband S, Yamamoto K, Yu J, Siang C, Jarvis ED. 2004. Revised nomenclature for avian telencephalon and some related brainstem nuclei. J Comp Neurol 473:377–414.
Rendahl H. 1924. Embryologische und morphologische. Studies über das Zwischenhirn beim Huhn. Acta Zool (Stockholm) 5:241–344.
Rubenstein JL, Shimamura K, Martínez S, Puelles L. 1998. Regionalization of the prosencephalon neural plate. Annu Rev Neurosci 21:445–477.
Selleck SB. 2000. Proteoglycans and pattern formation: sugar biochemistry meets developmental genetics. Trends Genet 16:206–212.
Shimamura K, Hartigan DJ, Martínez S, Puelles L, Rubenstein JL. 1995. Longitudinal organization of the anterior neural plate and neural tube. Development 121: 3923–3933.
Spassky N, Goujet-Zalc C, Parmantier E, Olivier C, Martinez S, Vanova A, Ikenaka K, Macklin W, Cerruti I, Zalc B, Thomas JL. 1988. Multiple restricted origin of oligodendrocytes. J Neurosci 18: 8331–8343.
Spassky N, Han YG, Aguilar A, Strehl L, Besse L, Laclef C, Ros MR, Garcia-Verdugo JM, Alvarez-Buylla A. 2008. Primary cilia are required for cerebellar development and Shh-dependent expansion of progenitor pool. Dev Biol 317:246–259.
Trousse F, Giess MC, Soula C, Ghandour S, Duprat AM, Cochard P. 1995. Notochord and floor plate stimulate oligodendrocyte differentiation in cultures of the chick dorsal neural tube. J Neurosci Res 41:552–560.
Vaillant C, Monard D. 2009. SHH pathway and cerebellar development. Cerebellum 18 [Epub ahead of print].
Vieira C, Garda AL, Shimamura K, Martinez S. 2005. Thalamic development induced by Shh in the chick embryo. Dev Biol 284:351–363.
Viviano BL, Paine-Saunders S, Gasiunas N, Gallagher J, Saunders S. 2004. Domain-specific modification of heparan sulfate by Qsulf1 modulates the binding of the bone morphogenetic protein antagonist Noggin. J Biol Chem 279: 5604–5611.
Wang S, Ai X, Freeman SD, Pownall ME, Lu Q, Kessler DS, Emerson CP Jr. 2004. QSulf1, a heparin sulfate 6-O-endosulfatase, inhibits fibroblasts growth factor signalling in mesoderm induction and angiogenesis. Proc Natl Acad Sci U S A 101:4833–4838.
Yoon MS, Puelles L, Redies C. 2000. Formation of cadherin-expressing brain nuclei in diencephalic alar plate subdivisions. J Comp Neurol 421:461–480.